PS-3-18
Extended Abstracts of the 2012 International Conference on Solid State Devices and Materials, Kyoto, 2012, pp100-101

Impact of Backgate Bias on the Sensitivity of Threshold Voltage to Process and Temperature Variations for Ultra-Thin-Body GeOI and InGaAs-OI MOSFETs Considering Quantum Confinement

Chang-Hung Yu and Pin Su
Department of Electronics Engineering & Institute of Electronics, National Chiao Tung University, Taiwan
E-mail: pinsu@faculty.nctu.edu.tw

Introduction

Germanium and III-V materials such as InGaAs have been proposed as channel material for future CMOS devices because of their enhanced transport properties [1-2]. The ultra-thin body (UTB) structure has been suggested to improve the device electrostatic integrity (EI) [3-4]. Using the UTB with thin BOX structure also enables backgate modulation of threshold voltage (V_{th}) [3-4] for power-performance optimization. With the scaling of device dimension, the quantum confinement (QC) effect may become significant. Whether the QC effect will impact the backgate-bias (V_{bg}) dependence of V_{th} sensitivity to process and temperature (T) variations for UTB GeOI and InGaAs-OI devices has rarely been known and merits investigation. In this work, using an analytical solution of Schrödinger equation verified with TCAD simulation, we investigate the impact of V_{bg} on the sensitivity of V_{th} to channel length (L), channel thickness (T_{ch}) and temperature variations for UTB GeOI and InGaAs-OI MOSFETs considering quantum confinement.

Methodology – Quantum-Confinement Model

Fig. 1 shows a schematic sketch of a UTB with thin BOX structure. To consider the QC effect along the T_{ch} direction, the Schrödinger equation can be solved by treating the wave function $\Psi_j(x)$ as power series and conduction band edge $E_C(x)$ as a parabolic form [5-6]. Assuming the boundary condition $\Psi_j(x = 0) = \Psi_j(x = T_{ch}) = 0$, the eigen-energies and wave functions of UTB MOSFETs under subthreshold region can be derived [5-6]. We have verified our model using the TCAD simulation that numerically solves the self-consistent solution of 2-D Poisson and 1-D Schrödinger equations [7]. Fig. 2 shows that the E_j's calculated by our model are fairly accurate. It should be noted that, as indicated in Fig. 2(b), the triangular potential well of V_{bg} = -1V is much sharper than that of V_{bg} = 1V, and thus the eigen-energies of V_{bg} = -1V are higher than the V_{bg} = 1V counterparts.

Sensitivity of V_{th} to Process Variations

In this study, we assume that the 3σ process variations of device parameters are ±10% of their nominal values, and use V_{th} variation $\Delta V_{th} = |V_{th}(+10\%) - V_{th}(-10\%)| / 2$ to represent the sensitivity of V_{th} to process variations [8].

Fig. 3 shows that, for both the GeOI and InGaAs-OI device, the ΔV_{th} caused by L variation ($\Delta V_{th,L}$) increases with increasing V_{bg} under the classical (CL) condition. This is because the device electrostatic integrity deteriorates as V_{bg} increases. However, after considering the QC effect, both the GeOI and InGaAs-OI devices show reduced sensitivity of $\Delta V_{th,L}$ to V_{bg}. In addition, the impact of QC on the InGaAs-OI device is larger than the GeOI counterpart due to its lower quantization effective mass. Fig. 4(a) shows that the V_{th} roll-off considering the QC effect is larger than the CL one for the GeOI device with V_{bg} = -1V, while Fig. 4(b) shows an opposite trend with V_{bg} = 1V. This explains why the QC effect suppresses the sensitivity of $\Delta V_{th,L}$ to V_{bg}. Fig. 5 shows that the (E_0–$E_{C,min}$) (and thus the QC-induced V_{th} shift) of the long-channel GeOI device (L=100nm) substantially reduces with increasing V_{bg} because of the V_{bg}-modulated triangular well (see Fig. 2(b)). This explains Fig. 4.

Fig. 6 shows that the ΔV_{th} caused by T_{ch} variation ($\Delta V_{th,Tch}$) increases with V_{bg} under CL condition for both the GeOI and InGaAs-OI device with T_{ch}=10nm because the carrier centroid moves from frontgate to backgate interface as V_{bg} changes from -1V to 1V. In addition, for a given V_{bg} (e.g. V_{bg}= -1V), the QC effect increases the $\Delta V_{th,Tch}$. Nevertheless, after considering the QC effect, the backgate-bias dependence of $\Delta V_{th, Tch}$ becomes weaker. In Fig. 7(a) with V_{bg} = -1V, the QC-induced V_{th} shift decreases as T_{ch} increases, and thus the sensitivity of V_{th} to T_{ch} around T_{ch}=10nm is enhanced by the QC effect. However, in Fig. 7(b) with V_{bg} = 1V, the QC-induced V_{th} shift is comparable around T_{ch}=10nm. This is because the (E_0–$E_{C,min}$) (and thus the QC-induced V_{th} shift) of V_{bg} = -1V decreases with increasing T_{ch}, while the (E_0–$E_{C,min}$) of V_{bg} = 1V is saturated around T_{ch}=8nm, as indicated in Fig. 8.

Sensitivity of V_{th} to Temperature Variation

Fig. 9 shows that the sensitivity of V_{th} to T ($|\Delta V_{th}/\Delta T|$) increases with V_{bg} under CL condition for both the GeOI and InGaAs-OI devices. It can also be seen that, for a given V_{bg} (e.g. V_{bg}= -1V), the $|\Delta V_{th}/\Delta T|$ is increased by the QC effect. Moreover, for a given V_{bg}, the QC-increased $|\Delta V_{th}/\Delta T|$ of the InGaAs-OI device is larger than the GeOI counterpart. However, as the QC effect is considered, the sensitivity of $|\Delta V_{th}/\Delta T|$ to V_{bg} is reduced. Fig. 10 indicates that the QC-induced V_{th} shift at T=200K is larger than that at T=400K for V_{bg} = -1V, while they are comparable for V_{bg} = 1V. This may be explained by the dominance of electrical confinement as V_{bg} decreases due to the sharper triangular well of V_{bg} = -1V. Therefore, the sensitivity of $|\Delta V_{th}/\Delta T|$ to V_{bg} considering the QC effect is reduced (see Fig. 9).

Summary

Using an analytical solution of Schrödinger equation verified with TCAD simulation, we demonstrate that the QC effect significantly reduces the backgate-bias dependence of the V_{th} sensitivity to process and temperature variations. Since Ge and InGaAs channels exhibit different degree of quantum confinement (due to different quantization effective mass), the impact of quantum confinement has to be considered when one-to-one comparisons between GeOI and InGaAs-OI MOSFETs regarding variability are made. Our study may provide insights for multi-V_{th} device/circuit designs using advanced UTB technologies.

Acknowledgement

This work was supported in part by the National Science Council of Taiwan under contract NSC 100-2628-E-009-024-MY2, and in part by the Ministry of Education in Taiwan under ATU program.

References

[1] S. Bedell *et al.*, *IEEE EDL*, vol. 29, no. 7, pp. 811, 2008.
[2] M. Radosavljevic *et al.*, *IEDM Tech. Dig.*, pp. 319, 2009.
[3] F. Andrieu *et al.*, *Symp. VLSI Tech*., pp. 57, 2010.
[4] C. Fenouillet-Beranger *et al.*, *Symp. VLSI Tech*., pp. 65, 2010.
[5] Y. Wu *et al.*, *IEEE EDL*, vol. 32, no. 1, pp. 18, 2011.
[6] C. Yu *et al.*, *IEEE TNANO*, vol. 11, no. 2, pp. 287, 2012.
[7] *ATLAS User's Manual*, SILVACO, 2008.
[8] T. Ohtou *et al.*, *IEEE EDL*, vol. 28, no. 8, pp. 740, 2007.

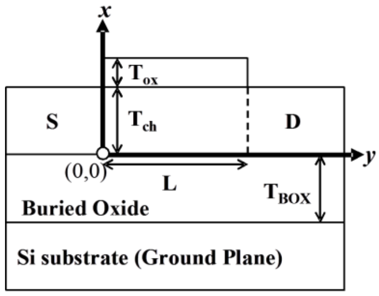

Fig. 1. Schematic sketch of a UTB structure with thin BOX. The origin point is located at the channel/BOX interface of source/channel junction. L is the channel length. T_{ch}, T_{ox} and T_{BOX} are thicknesses of channel, gate oxide and BOX, respectively.

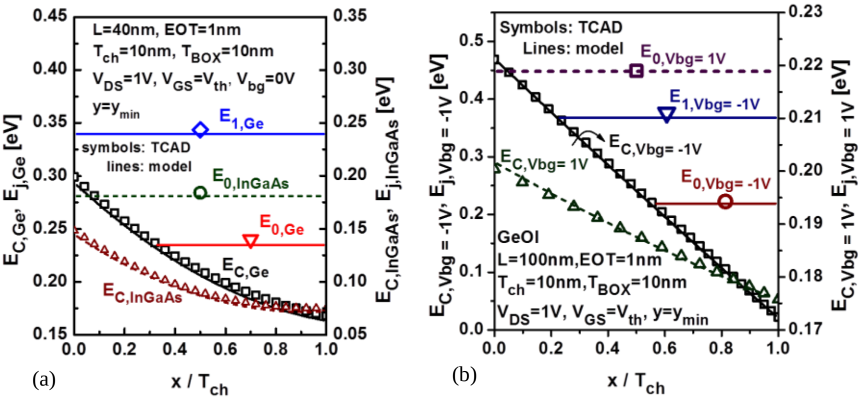

Fig. 2. Conduction band edge E_C and quantized eigen-energies of UTB MOSFETs. (a) Short-channel GeOI and InGaAs-OI devices with parabolic well at V_{bg} = 0 V. (b) Long-channel GeOI device with triangular potential well for V_{bg} = -1 V and V_{bg} = 1 V.

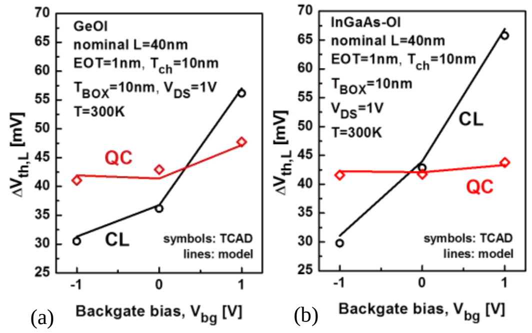

Fig. 3. Comparison of the sensitivity of $\Delta V_{th,L}$ to V_{bg} with and without considering the QC effect for short-channel UTB GeOI and InGaAs-OI devices. $\Delta V_{th,L}$ denotes the V_{th} variation caused by the L variation. CL: classical condition.

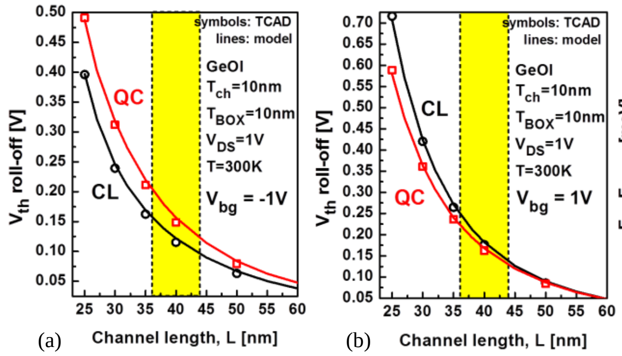

Fig. 4. The V_{th} roll-off is defined as V_{th}(L = 100 nm) – V_{th}(L). Comparison of the V_{th} roll-off between QC and CL for the UTB GeOI device with T_{ch} = 10 nm. (a) V_{bg} = -1V. (b) V_{bg} = 1V.

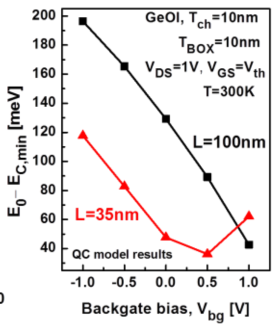

Fig. 5. Impact of V_{bg} on the ground-state eigen-energy (E_0–$E_{C,min}$) of long-channel and short-channel UTB GeOI devices with T_{ch} = 10 nm.

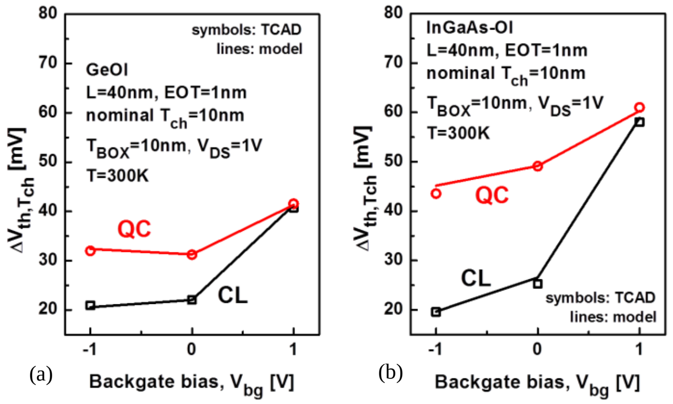

Fig. 6. Comparison of the sensitivity of $\Delta V_{th,Tch}$ to V_{bg} with and without considering the QC effect for short-channel UTB GeOI and InGaAs-OI devices. $\Delta V_{th,Tch}$ denotes the V_{th} variation caused by the T_{ch} variation.

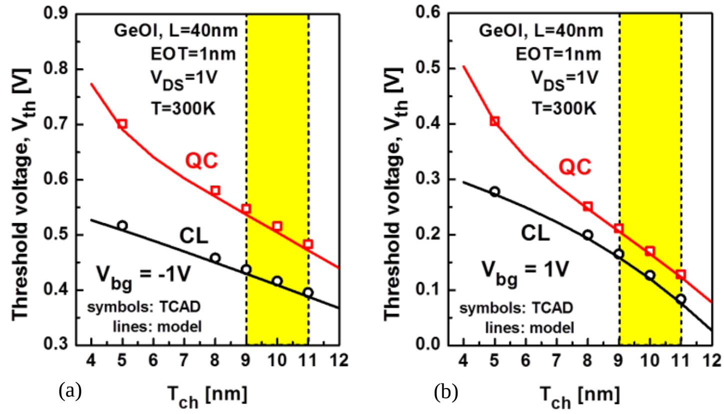

Fig. 7. Impact of quantum confinement on the sensitivity of V_{th} to T_{ch} for short-channel UTB GeOI devices with various T_{ch}. (a) V_{bg} = -1V. (b) V_{bg} = 1V.

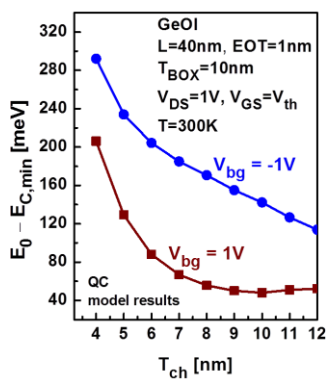

Fig. 8. The difference of ground-state eigen-energy (E_0–$E_{C,min}$) between V_{bg} = -1V and V_{bg} = 1V with various T_{ch} for a short-channel UTB GeOI device.

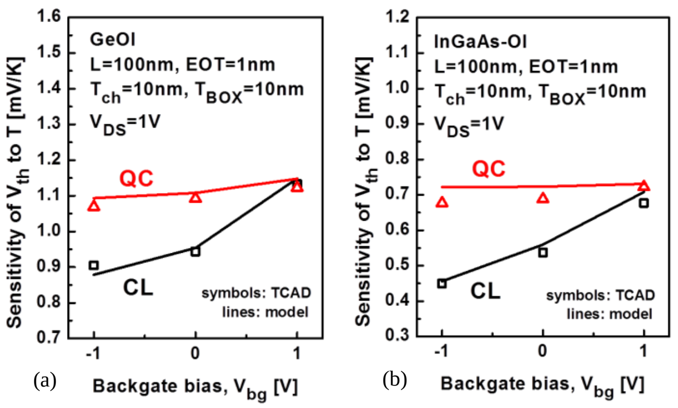

Fig. 9. Comparison of the V_{bg} dependence of the V_{th} sensitivity to temperature between the QC and CL for long-channel UTB GeOI and InGaAs-OI devices. The sensitivity of V_{th} to temperature ($|\Delta V_{th}/\Delta T|$) is defined as $|V_{th}(T = 400K)–V_{th}(T = 200K)|/(400K – 200K)$.

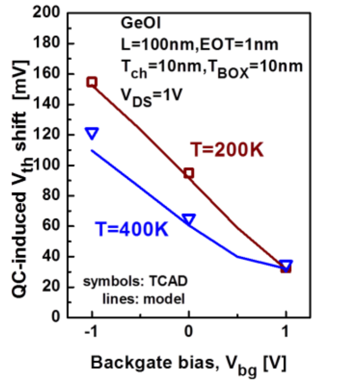

Fig. 10. The difference of QC-induced V_{th} shift between T = 200 K and T = 400 K with various V_{bg} for a long-channel UTB GeOI device.